Digest Journal of Nanomaterials and Biostructures Vol. 6, No. 3, July – September 2011, p 953 -959

FABRICATION OF BST NANO-CERAMICS BY TWO-STEP SINTERING

XI-LIN WANG[*], YU-ZHEN ZHAO, YONG-JIE, ZHAO, SHAN-SHAN LIU, HE-PING ZHOU
State Key Laboratory of New Ceramics and Fine Processing, Department of Materials Science and Engineering, Tsinghua University, Beijing, China, 100084

$Ba_xSr_{1-x}TiO_3$ [(BST), $0\leq x\leq 1$] is a solid solution ferroelectric material exhibiting a large dielectric constant non-linear change with an applied DC electric field. In this paper, $Ba_{0.6}Sr_{0.4}TiO_3$ ceramic was obtained by traditional ceramic processing and two-step sintering. The structural, surface morphological, dielectric properties, tunable properties of this material as well as the mechanism of their nonlinear dielectric constant under DC electric field were systematically examined. The grain size of samples fabricated by two-step sintering was about 300-500nm, while the average grain size of samples by traditionally sintered was 20μm. X-ray diffraction analyses indicated that the samples present perovskite phase. Scanning electron microscopy micrograph of sample indicated that the density increased to 97%. The kinetics of two-step sintering is also discussed, exploring the difference between densification diffusion and grain boundary mobility. The two-step sintered samples presented lower dielectric constant and dielectric loss than samples by traditionally sintered.

(Received May 5,2011; Accepted May 17, 2011)

Keywords: BST, Tunablilty, two-step sintering

1. Introduction

Barium strontium titanate (Ba,Sr)TiO_3 (short for BST) ferroelectric material with high dielectric constant is one of the promising candidates for high-frequency tunable devices and dynamic random access memory (DRAM) applications[1]. For its strong response to the applied electric filed, BST has been used to develop devices operating in microwave such as tunable capacitors, phase shifters, and frequency agile filters. These materials are characterized by two parameters, 1) tunability[1]:

$$n=\varepsilon_{(0)}/\ \varepsilon_{(\mathrm{Emax})} \tag{1}$$

Or relative tunability:

$$n_r=(\varepsilon_{(0)}-\ \varepsilon_{(\mathrm{Emax})})/\ \varepsilon_{(0)} \tag{2}$$

Where $\varepsilon_{(0)}$ and $\varepsilon_{(\mathrm{Emax})}$ are dielectric constants of the material at zero and the maximum bias electric field respectively; 2) loss tangent (tanδ).

There are many reports studying the dielectric and tunable properties of ferroelectric BST materials by the monotonous dependence of its dielectric and ferroelectric properties on the Ba/Sr ratio [2-5]. Generally, $Ba_{0.6}Sr_{0.4}TiO_3$ was chosen as the basic composition because of its good dielectric properties and tunability. However, the high dielectric loss limits its further development, especially in the microwave frequency range. To improve the dielectric properties of BST for phased array applications, it is necessary to lower dielectric constant and loss tangent.

---

[*] Corresponding author: wangxiliin@hotmail.com

The recent development of an unconventional two-step sintering strategy featuring densification without grain growth is deemed particularly exciting as reported in Nature[6], since it promises to deliver nanoceramics by pressureless sintering. The success of two-step sintering is determined by the pore morphology of the material prior to low-temperature second-stage sintering.

In this paper, more effort has been done to fabricate bulk dense BST ceramics from submicron down to nanometer size using the two-step sintering method, and the dielectric properties of the samples were also examined.

2. Experimental procedures

$Ba_{0.6}Sr_{0.4}TiO_3$ ceramics were synthesized by the conventional solid-state reaction method and two-step sintering method. The starting materials were $BaCO_3$(purity of 99.95%), $SrCO_3$ (purity of 99.95%), TiO_2(purity of 99.95%), and ZrO_2(purity of 99.95%). For traditional solid-state reaction sintering, these materials were mixed in a ball mill with ethanol, then dried and calcined in an alumina crucible at 1100℃for 2 h in air. The calcined powder was remilled with a 4 wt.% polyvinyl butyral as a binder. Uniaxial pressing with 200 Mpa pressed the dried powders to get pellets with 10 mm diameter and 1–2 mm thick. These pellets were sintered in air at 1400℃for 2h. The heating and cooling rate were 5℃/min.

For two-step sintering, the powders of BST were prepared by sol-gel, and then remilled with a 4 wt.% polyvinyl butyral as a binder. After isostatic pressing at 200 MPa to achieve a relative density of 46%, the green compacts were sintered using various two-step firing schedules (showed in fig 1.). Typically, the sample was heated at 30 °C/min to a higher temperature T_1 (1,400–1,450 °C), then immediately cooled, at 20 °C/min, to a lower temperature T_2 (1,200–1,250 °C) for isothermal sintering with times of 10-24 h. The two-step schedules of sample 1 to sample 6 were listed in tableⅠ.

The bulk density of the samples was measured by Archimedes method. X-ray diffraction (CuK_radiation D/MAX 2500, Rigaku) was carried out on samples for phase identification. The microstructures were observed using scanning electron microscopy (model SEM, LEO-1530, Oberkochen, Germany). Silver paste electrodes were painted on both sides of sintered ceramic specimens for dielectric and ferroelectric measurements. The capacitance and loss tangent(tanδ) of the samples were measured using impedance analyzer (HP4192A) in the frequency of 100 kHz. Dielectric properties were measured in the temperatures range from -50°C to 150°C. The dielectric tunability were measured using a TH2816 LCR testing meter (TH2816, Tonghui Electric, China) under the DC bias electric field from 0 to 1.5 kV/mm in the frequency of 100 kHz.

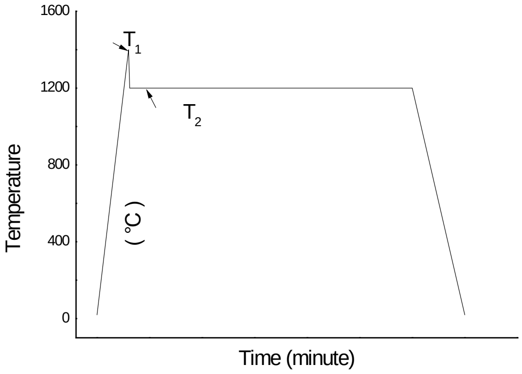

Fig 1. Two-step sintering temperature program schedule.

TableI. two-step sinteing of $Ba_{0.6}Sr_{0.4}TiO_3$ *ceramics.*

Sample	T_1(℃)	T_2 (℃)	Sintering time(h)
0*	1400	1400	2
1	1450	1250	10
2	1400	1200	12
3	1400	1200	15
4	1400	1200	24
5	1400	1250	10
6	1400	1250	20

* (traditional sintering)

3. Results and discussion

In two-step sintering, the samples are quickly heated first to a higher temperature, T_1, to obtain certain low grain size, and then sintered at a lower temperature T_2 for some time (thermal cycle as shown in Fig. 1 insert and Table I) to reach high density. During the second sintering step, density improved from a lower value to better than 98% without any grain growth. This two-step schedule is very different from the conventional process in ceramic sintering.

Usually, in conventional sintering, the nanosized BST green compacts are heated in a first cycle at a predetermined rate, and held at desired temperature until the highest densification level is reached. The average grain size of samples via this way increases continuously as density increases. The grain size of the dense BST ceramic sintered at 1,400 °C/2 h (93%) by conventional sintered is 20 μm.

In two step process, a sufficiently high starting density has been obtained during the first stage. The free energy of ceramic surface remains very high and could deliver adequate energy to complete densification during the second stage. In BST system, the critical density obtained at T_1, which is required for producing dense ceramics during the second step sintering, is about 73%. It is found that the temperature T_2 required for the second step decreased with the increasing grain size. However, if T_2 is too low, then sintering proceeds for a while and then becomes exhausted. On the other hand, if T_2 is too high, grain growth still occurs in the second step.

Figure 2 shows X-ray diffraction spectra for $Ba_{0.6}Sr_{0.4}TiO_3$ ceramics by different sintering method. The sintered ceramics are single phase of perovskite structure. The position of the peaks of two-sintered samples in XRD there is no shift, but the peaks are evidently broader than that of conventional sintering sample.

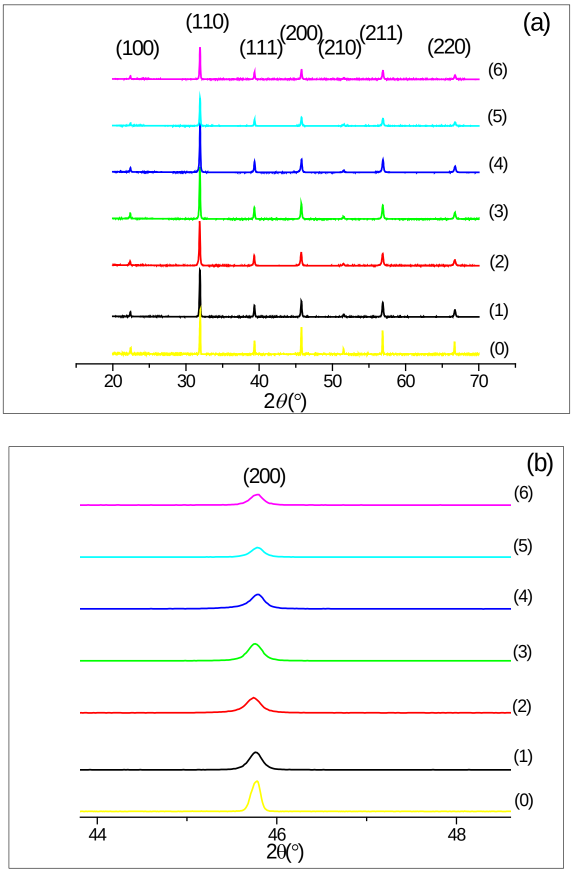

Fig 2. X-ray diffraction patterns of $Ba_{0.6}Sr_{0.4}TiO_3$ ceramics sintered by two-step sintering and traditional sintering (a) continuous scanning , (b)step-scanning.

Table II shows the average grain size and density of samples obtained by two sintering methods, and SEM photos of samples prepared by two sintering methods was exhibinted in figure 3. The grain sizes in table II are consistent with XRD results. For the nano-size of the two-step sintering samples, the (200) peaks was broader than that of conventional sintering sample.

The grain sizes of two-step sintered sample and conventional sintered sample were 0.30-0.47μm and 20μm, respectively. Measured by the Archimedes method, the densities of the sample 1 and sample 0 are 5.61g/cm^3(TD=5.69g/cm^3), 5.32g/cm^3, respectively. In two-step sintering, the higher the T_1 and the bigger the grain size, and the time held in T_2 was longer and the samples was more dense.

Table II grain size and density of samples prepared by two sintering methods

Sample	Grain size (μm)	Estimated density (g/cm^3)	Sintered density (%)
0	20	5.32	93.66
1	0.47	5.61	98.76
2	0.30	5.21	91.72
3	0.31	5.33	93.83
4	0.33	5.46	96.12
5	0.40	5.14	90.49
6	0.43	5.18	91.19

In two-step sintering, to achieve densification without grain growth, grain boundary diffusion needs to be maintained while the grain boundary migration suppressed and the sintering temperature held in T_2. The grain boundary migration involves additional kinetic processes other than grain boundary diffusion, and if such processes require a higher activation energy, then grain boundary migration can be suppressed at lower temperature despite active grain boundary diffusion. The most likely candidates for such step are the movement of nodal points or nodal lines on the grain boundary, such as four-grain junctions, pore-grain boundary junctions, or three-grain junctions (lines)[7] .

Although theoretical models usually employ idealized geometric assumptions which may not hold in real materials[8-10] , general dimensional argument originated by Herring[11] states that the normalized rate of densification, via grain boundary diffusion, can be expressed as

$$\mathrm{d}\rho/\rho\mathrm{d}t = F_{(\rho)}(\gamma\Omega/GkT)(\delta \mathrm{D}/\mathrm{G}^3) \qquad (3)$$

where t is the time, g is the surface energy, Ω is the atomic volume, k is the Boltzmann constant, T is the absolute temperature, G is the mean grain diameter, d is the width of the grain boundary, D is the grain boundary diffusivity, and F(r) is an unspecified function of density r. This argument holds for different grain size and density provided the sintering microstructure, including the pore distribution, is a function of density only once the length scale is renormalized by the grain size[6]. For a ceramic undergoing two-step sintering, the grain boundary network is frozen, so there is no change in microstructure other than the shrinking porosity.

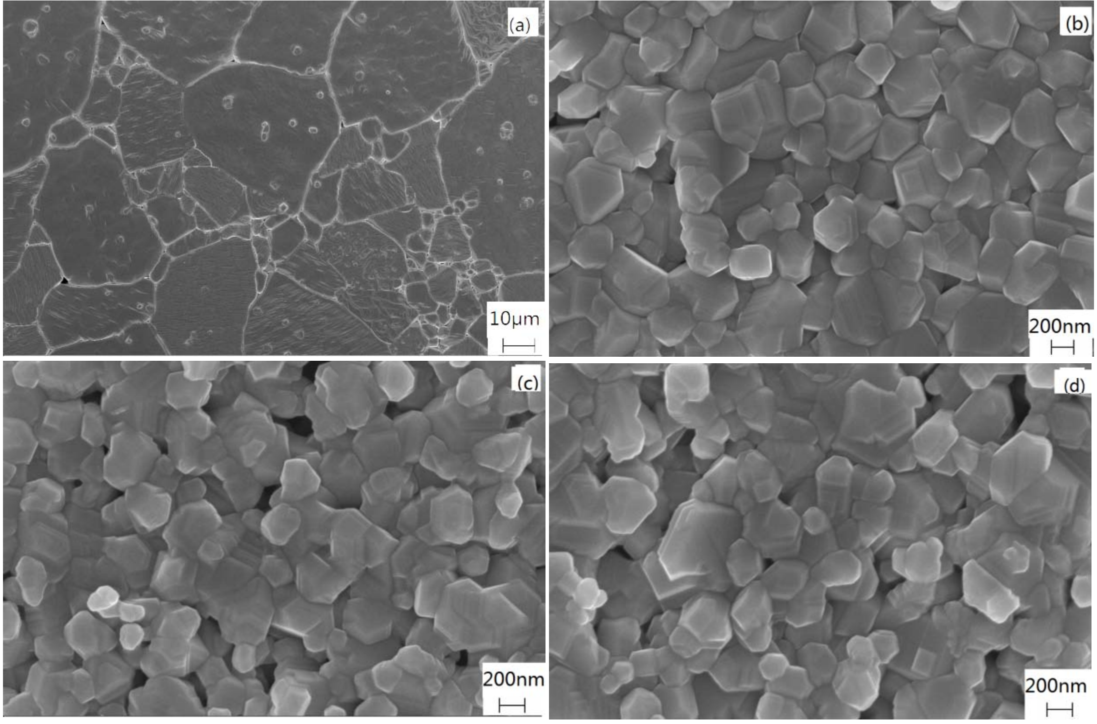

Fig 3. SEM photos of samples prepared by two sintering methods
(a)Sample 0 , (b)Sample 1 , (c) Sample 2 , (d) Sample 5

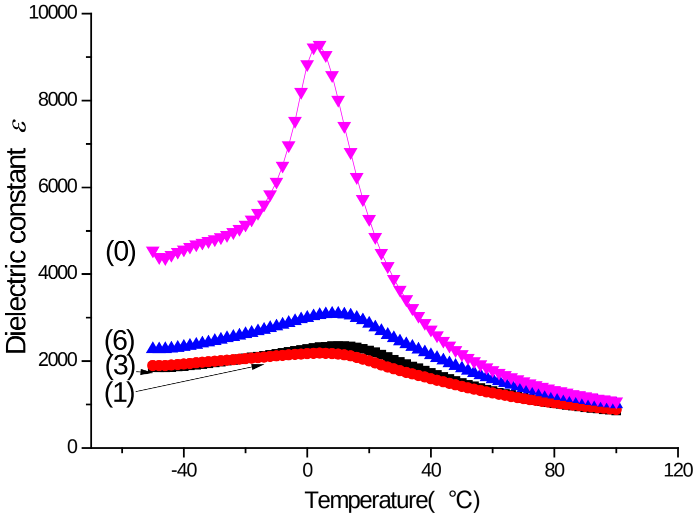

Fig 4. Dielectric constant of samples verse temperature.

It is noticed that two-step sintering significantly depresses and broadens phase transition peak of BST ceramics (Fig. 4), and the dielectric constant at the phase transition peak was reduced from 9500 to 2100. As the grain sizes of samples decrease, the dielectric constant decreases. The phase transition temperature is near 0℃. Dielectric frequency dispersion is very evidently clear because grain sizes of samples in the two-step sintering are nanometers, while mass diffusion and transfer are not enough compared to traditional sintering, the constituents of micro-area fluctuate at a large scale and the samples exhibit phase transition disperson at macro level.

Table III shows the dielectric properties of the samples under DC bias field at 100kHz. The dielectric constant and dielectric loss of samples by two-step sintered was obviously lower than that of prepared by traditional sintering. But the dielectric tunability of samples by two-step is worse than that of conventional sintering, and the highest value 19.34% in all the samples prepared by two-step sintering was achieved in sample 1.

Table III Dielectric properties of samples(100 kHz, 1.5 kV/mm)

Sample	Dielectric constant	Dielectric loss	Tunability (%)
0	4908	0.00943	34.61
1	1977	0.00472	19.34
2	1596	0.00728	13.38
3	1926	0.00616	15.11
4	1999	0.00728	16.19
5	1734	0.00501	12.13
6	2438	0.00488	17.52

The decreasement of dielectric constant and dielectric loss of samples by two-step sintered should be attributed to two factors, grain size of nanometer and distortion of crystal lattice caused by two-step sintering.

The interpretation of dielectric nonlinearity of BST in paraelectric state is related to polar nano-region[12-15] . The concept of polar nano-region is more precise than polarmicroregion (a.b. PMR) on account of their nanometer scale. Polar nano-region was defined as nanometer scale region with parallel oriented spontaneous polarization, where they consists of each other acting as a giant dipole with slow relaxation frequency. The polar nano-region is susceptive to environmental disturbance and apt to redirect to external field vector even under weak signal level. Dielectric nonlinearity can be manifestly understood under the assumption that polar nano-region losses its susceptibility while merging into micro domain or macro domain if applied external bias field is strong enough.

4. Conclusion

Two-step pressureless sintering was used to prepare $Ba_{0.6}Sr_{0.4}$TiO3 ceramics possessing high density with ultrafine grain size. The samples obtained by two-step sintering exhibited better dielectric tunable properties than conventional sintering samples. Reduced the dielectric constant and dielectric loss, were obtained in two-step sintering samples, due to its high densification and fine grain. The room temperature dielectric constant, dielectric loss, relative dielectric tunablity and at 100kHz are 1977, 0.0047, and 20%, respectively.

Acknowledgements

The authors thank the National Science Fund of China (Grant No. 50572050).

Reference

[1] A. Tagantsev, V. Sherman, K. Astafiev, J. Venkatesh, and N. Setter, Journal of Electroceramics 11 (2003) 5.

[2] V. V. Lemanov, E. P. Smirnova, P. P. Syrnikov, E. A. Tarakanov, Physical Review B **54**, 3151 (1996).

[3] A. Hilton and B. Ricketts, Journal of physics. D, Applied physics **29**, 1321 (1996).

[4] V. Shut, S. Syrtsov, and V. Trublovsky, Phase Transitions **83**, 368 (2010).

[5] X. L. Wang, H. Xue, and H. P. Zhou, Rare Metal Materials and Engineering **36**, 935 (2007).

[6] I. W. Chen, X. H. Wang, Nature **404**, 168 (2000).

[7] I. W. Chen, Interface Science **8**, 147 (2000).

[8] G. N. Hassold, I. W. Chen, D. J. Srolovitz, Journal of the American Ceramic Society **73**, 2857 (1990).

[9] I. W. Chen, G. N. Hassold, D. J. Srolovitz, Journal of the American Ceramic Society **73**, 2865 (1990).

[10] D. L. Zhang, G. A. Weng, S. P. Gong, and D. X. Zhou, Materials Science and Engineering B-Solid State Materials for Advanced Technology **99**, 428 (2003).

[11] C. Herring, Journal of Applied Physics **21**, 301 (1950).

[12] X. Yao, Z. Chen, L. E. Cross, Journal of Applied Physics **54**, 3399 (1983).

[13] X. Yao, Z. L. Chen, L. E. Cross, Ferroelectrics **54**, 503 (1984).

[14] Q. Xu, X. F. Zhang, Y. H. Huang, W. Chen, H. X. Liu, M. Chen, B. H. Kim, Journal of Alloys and Compounds **485**, L16 (2009).

[15] Q. Xu, X. F. Zhang, Y. H. Huang, W. Chen, H. X. Liu, M. Chen, B. H. Kim, Journal of Physics and Chemistry of Solids **71**, 1550 (2010).